Measuring Extreme Vacuum Pressure with Ultraintense Lasers

Angel Paredes,[1] David Novoa,[2] and Daniele Tommasini[1]

[1]*Departamento de Física Aplicada, Universidade de Vigo, As Lagoas, Ourense ES-32004, Spain*

[2]*Centro de Láseres Pulsados, CLPU. Edificio M3-Parque Científico, Calle del Adaja, Villamayor ES-37185, Spain*

(Received 8 June 2012; revised manuscript received 4 October 2012; published 20 December 2012)

We show that extreme vacuum pressures can be measured with current technology by detecting the photons produced by the relativistic Thomson scattering of ultraintense laser light by the electrons of the medium. We compute the amount of radiation scattered at different frequencies and angles when a Gaussian laser pulse crosses a vacuum tube and design strategies for the efficient measurement of pressure. In particular, we show that a single day experiment at a high repetition rate petawatt laser facility such as Vega, that will be operating in 2014 in Salamanca, will be sensitive, in principle, to pressures p as low as 10^{-16} Pa, and will be able to provide highly reliable measurements for $p \gtrsim 10^{-14}$ Pa.

DOI: 10.1103/PhysRevLett.109.253903 PACS numbers: 42.62.−b, 07.30.Dz, 41.60.−m, 52.38.−r

Introduction.—Extreme-high vacuum (XHV) pressures, $p < 10^{-10}$ Pa [1], are usually measured by ionization methods: the atoms in the sample are ionized and the produced charged particles are collected by applying an electric field. This procedure is fully reliable for pressures as low as 10^{-11} Pa [2]. Although there are techniques able to push this limit down [3], its use would be questionable since in this regime the electron stimulated desorption, the so-called x-ray limit, or the outgassing from the hot cathode cannot be neglected [2,4]. It is therefore crucial to think of alternative methods to measure XHV below 10^{-11} Pa without significantly altering the pressure itself and free of the aforementioned limitations. One such possibility is to gauge the pressure by measuring the storage time of ions in a Penning trap, since their main loss mechanism comes from interaction with residual neutral particles [5].

In this Letter, we propose to use photons to gauge the extreme vacuum properties. The advent of ultrahigh intensity lasers [6] has provided a new class of light sources which are powerful enough to produce a measurable signal even in conditions of XHV, where the remnant pressure is essentially produced by the hydrogen released by the walls. When interacting with high-intensity laser light, the electrons can be considered as free, therefore the main source of dispersed light is nonlinear Thomson scattering. This process was studied in detail in Refs. [7–11] and experimentally observed in Ref. [12], and may be used to measure the peak intensity of a laser pulse [13].

XHV is a necessary requirement of many experiments based in ultraintense lasers that have been proposed in the last few years aimed at demonstrating the quantum vacuum polarization [14–17] and at searching for new particles [18]. Remarkably, the laser itself may provide an efficient tool to monitor the pressure, substituting or complementing other methods. XHV is also necessary in certain facilities such as LHC at CERN, where pressures around 5×10^{-11} Pa have been recently reported [19].

We will compute the number of scattered photons as a function of the electron density of the medium and the parameters of the ultraintense laser pulse. In the XHV regime, collective effects of the electrons as those discussed in Refs. [9,10] can be neglected. The number of scattered photons is proportional to the number of scattering centers, which is proportional to the pressure. Harmonics are generated in the scattering process. Even if most of the scattered photons correspond to the incident wavelength ($n = 1$), detection of photons with $n = 2, 3, \ldots$ may be possible and useful.

Relativistic Thomson scattering.—Our computations are based on results of Ref. [8], which we briefly review. We introduce the dimensionless parameter q, related to the intensity I and wavelength λ_0 as

$$q^2 = \frac{2 I r_0 \lambda_0^2}{\pi m_e c^3}, \tag{1}$$

where $r_0 \approx 2.82 \times 10^{-15}$ m is the classical electron radius. Let us also define $\mathcal{M} = 1 + \frac{1}{2} q^2 \sin^2(\theta/2)$. Relativistic effects play a role for $q \gtrsim 1$, corresponding to $I \gtrsim 2 \times 10^{18}$ W/cm^2 (for $\lambda_0 = 800$ nm). When a linearly polarized plane wave impinges on a free electron (see Fig. 1), the power scattered per unit solid angle is $\frac{dP^{(n)}}{d\Omega} = \frac{e^2 c}{8 \epsilon_0 \lambda_0^2} f^{(n)}$, where n is the harmonic number and

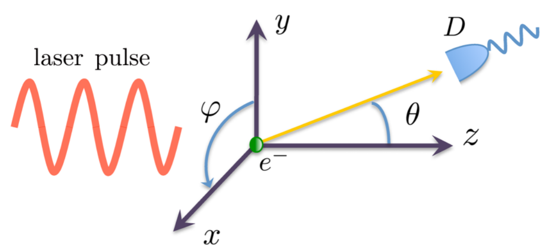

FIG. 1 (color online). Sketch of the system. The laser pulse impinges on the electron, initially located at the coordinate origin. The scattered radiation is observed on the detector D. The incoming pulse is linearly polarized along the y axis.

$$f^{(n)} = \frac{q^2 n^2}{\mathcal{M}^4}\left[\left(1 - \frac{(1+\frac{1}{2}q^2)\cos^2\alpha}{\mathcal{M}^2}\right)(F_1^n)^2 - \frac{q\cos\alpha[\cos\theta - \frac{1}{2}q^2\sin^2(\theta/2)]}{2\mathcal{M}^2}F_1^n F_2^n + \frac{q^2\sin^2\theta}{16\mathcal{M}^2}(F_2^n)^2\right], \tag{2}$$

with $\cos\alpha = \sin\theta\cos\varphi$, where $\theta \in [0, \pi]$, $\varphi \in [0, 2\pi]$ are usual spherical coordinates. Forward scattering corresponds to $\theta = 0$ and $\varphi = 0$, π point along the polarization axis. The F_s^n can be written in terms of Bessel functions as $F_s^n = \sum_{l=-\infty}^{+\infty} J_l(\frac{nq^2\sin^2(\theta/2)}{4\mathcal{M}})[J_{2l+n+s}(\frac{qn\cos\alpha}{\mathcal{M}}) + J_{2l+n-s}(\frac{qn\cos\alpha}{\mathcal{M}})]$. These results hold in the laboratory frame, in which the scattered wavelength is shifted as $\lambda^{(n)} = \mathcal{M}\lambda_0/n$.

Modeling a realistic situation.—Our goal is to compute the average number of photons scattered when a laser pulse traverses a vacuum chamber. We model the pulse as having a Gaussian profile of intensity $I = I_0(\frac{w_0}{w(z)})^2 e^{-2r^2/w(z)^2}$. The beam width evolves as $w(z) = w_0\sqrt{1 + z^2/z_R^2}$, where the Rayleigh length is $z_R = \pi w_0^2/\lambda$. The average number of photons of the nth harmonic produced by a single pulse is $N_\gamma^{(n)} = n_e\tau\int\frac{dP^{(n)}}{d\Omega}\frac{\mathcal{M}\lambda}{hcn}d\Omega d^3\vec{x}$, where n_e is the electron density and τ is the pulse duration. It is useful to define dimensionless quantities $\rho \equiv r/w_0$, $\xi \equiv z/z_R$, such that

$$q^2 = q_0^2\frac{1}{1+\xi^2}\exp\left(-\frac{2\rho^2}{1+\xi^2}\right), \tag{3}$$

where q_0 is related to the intensity at the beam focus. After simple manipulations one can write

$$N_\gamma^{(n)} = \mathcal{K}\iint\rho\Gamma^{(n)}(q)d\rho d\xi, \tag{4}$$

where we have introduced a function $\Gamma^{(n)}(q) = \int_0^{2\pi}\int_0^{\pi} n^{-1} f^{(n)}\mathcal{M}\sin\theta d\theta d\varphi$, and the parameter $\mathcal{K} = \frac{1}{2}n_e c\tau\pi^2 w_0^4\lambda_0^{-2}\alpha$, where $\alpha \approx \frac{1}{137}$ is the fine structure constant. The integral in Eq. (4) only depends on n and q_0, whereas the rest of the quantities describing the physical situation are factored out in $\mathcal{K}$.

We have computed the number, frequency, and spatial distribution of the photons produced as a function of the incoming laser pulse parameters, by numerical integration of the expression (4). Figure 2 shows a plot of $\Gamma_n(q)$ for $n = 1, \ldots, 4$. Since it is impossible to have a detector covering the full solid angle, we also show the results when the integral is performed over a reduced range of the polar angle $\theta \in (\theta_{\rm cut}, \pi - \theta_{\rm cut})$. In a realistic situation, $\theta_{\rm cut}$ should be a function of ρ, ξ, φ, depending on the actual geometry, but for simplicity we illustrate the situation fixing a constant $\theta_{\rm cut}$. In any case, one should have $\theta_{\rm cut} \gg \theta_d$, being $\theta_d = \lambda_0/(\pi w_0)$ the beam divergence.

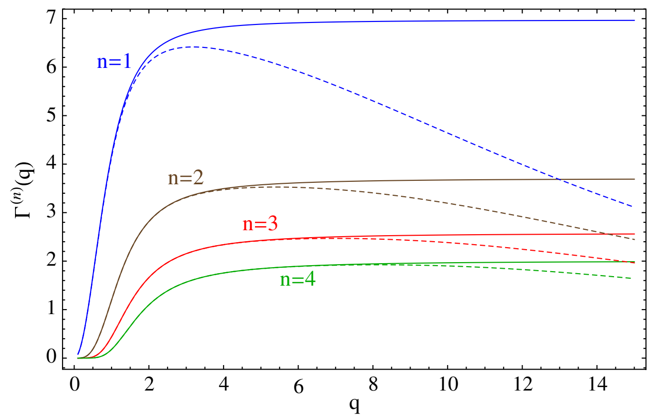

FIG. 2 (color online). In solid lines, the function $\Gamma^{(n)}(q)$ found by numerical integration. Dashed lines are found by cutting the θ-integration with $\theta_{\rm cut} = 0.1$.

Using these results for $\Gamma^{(n)}(q)$ and Eq. (3), one can compute the integral in (4), see Fig. 3. The integral was confined to the region where an electron of a hydrogen atom can be treated as free $q > q_{\rm cut} = 0.01$. For large enough q_0 (depending on n), one finds:

$$N_\gamma^{(n)} \approx c_n\mathcal{K}q_0^3, \tag{5}$$

with the values $c_1 \approx 275$, $c_2 \approx 1.3$, $c_3 \approx 0.22$, $c_4 \approx 0.088$. If for Fig. 3 one performs the same cut as before in the integration region $0.1 < \theta < \pi - 0.1$, the correction to the result is tiny, below 1%. This happens because most of the photons are *not* generated at the maximum intensity region, but at the larger volume where the Gaussian profile presents moderate values of q. In particular, for $n = 1$ most of the photons are generated in a region with $q < 1$ and therefore one can find an approximation to the $n = 1$ result, $c_1 \approx 8\pi/(9q_{\rm cut})$, using the expressions for nonrelativistic Thomson scattering.

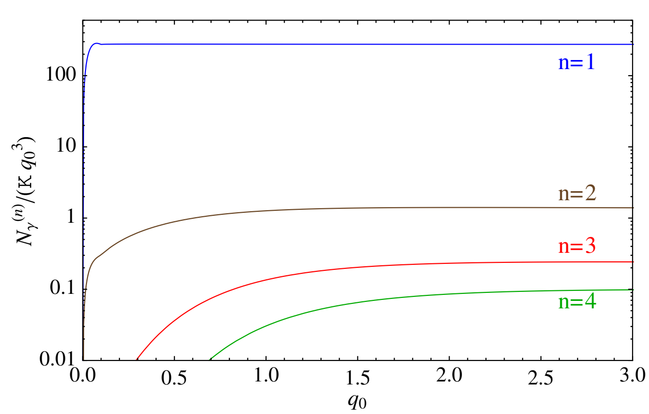

FIG. 3 (color online). Plot of the number $N_\gamma^{(n)}$ of photons of harmonic n produced by a single pulse as a function of its peak intensity. For illustrative purposes, what is actually shown is a semi-logarithmic plot of the dimensionless quantity $N_\gamma^{(n)}/\mathcal{K}q_0^3$ as a function of q_0 for $n = 1, 2, 3, 4$.

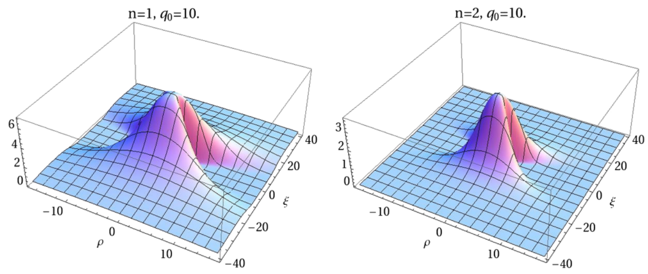

FIG. 4 (color online). The function $\Gamma^{(n)}(q(\rho, \xi))$, showing the region in space where the scattered radiation is produced, is plotted in two cases. For $n > 1$, photons are produced in the region where $q \gtrsim 1$. The region where $n = 1$ photons are scattered is larger since they are the only outcome of the non-relativistic regime $q \ll 1$.

In order to understand qualitatively the results for $n > 1$, we may approximate the plateaus of $\Gamma^{(n)}(q)$ displayed in Fig. 2 by Heaviside step functions $\Gamma^{(n)}(q) = b_n \Theta(q - q_{\text{step},n})$. Then, defining the limits of the $q > q_{\text{step},n}$ region as $\rho_{\text{lim}} = \sqrt{[(1 + \xi^2)/2] \log(q_0^2/q_{\text{step},n}^2(1 + \xi^2))}$ and $\xi_{\text{lim}} = \sqrt{(q_0^2/q_{\text{step},n}^2) - 1}$, one can estimate the integral in Eq. (4) as $\int_{-\xi_{\text{lim}}}^{\xi_{\text{lim}}} \int_0^{\rho_{\text{lim}}} \rho b_n d\rho d\xi \approx \frac{b_n q_0^3}{9 q_{\text{step},n}^3}$ where we have only kept the leading term in $q_0/q_{\text{step},n}$. This simplified analysis fits qualitatively the numerical results and explains the cubic dependence in q_0: it is a consequence of the fact that, roughly, both ρ_{lim}, ξ_{lim} grow linearly with q_0.

In Fig. 4, we present plots displaying the spatial region in which the photons are scattered, thus providing information about the precise region of the chamber where the electron density measurement is taking place.

Figure 5 exhibits two examples of the angular distribution of the emitted photons, obtained by performing the integral in (4) on the ρ-ξ space. For a given harmonic, the angular dependence does not change much when modifying q_0. The reason is that—as noted above—even when q_0 is large, a copious amount of radiation comes from the region of smaller q. This same argument explains why the distributions are not forward peaked, as one may naively expect. The plot for $n = 1$ can hardly be distinguished from the angular distribution corresponding to linear Thomson scattering $\sin\theta(1 - \sin^2\theta\cos^2\varphi)$. This is in sharp contrast with the result for an incoming plane wave (see, e.g., Ref. [11]) and highlights the importance of taking into account the spatial energy distribution.

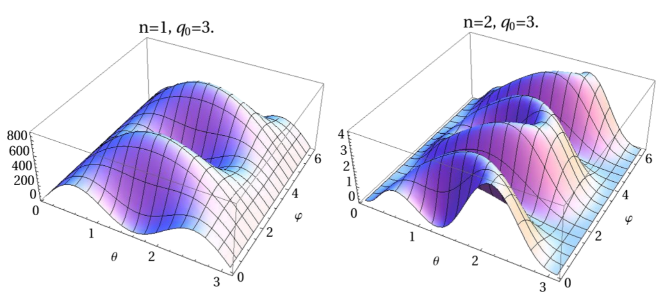

FIG. 5 (color online). Angular distribution of the scattered photons: plots of $(1/n) \iint \rho f^{(n)} \mathcal{M} \sin\theta d\rho d\xi$ as a function of θ and φ, see Eq. (4).

The spectral distribution of the scattered radiation can also be computed [20].

Quantitative estimates.—Using Eq. (5), we can estimate the number of photons detected in a time span Δt in terms of the laser repetition rate r_r, the total energy of each pulse $E_{\text{pulse}} = \tau I_0 \pi w_0^2/2$ and the detector efficiency f—which includes geometric and quantum factors.

$$N_{\gamma,\text{det}}^{(n)} \approx \frac{4c_n}{\pi}(\Delta t r_r) f \frac{\eta p}{k_B T} \alpha \frac{w_0 \lambda_0 r_0^{3/2}}{(c\tau)^{1/2}} \left(\frac{E_{\text{pulse}}}{m_e c^2}\right)^{3/2}, \quad (6)$$

where $p = n_e k_B T/\eta$ is the pressure, with η being the average number of weakly bound electrons per molecule. For fixed energy, the signal grows with the waist radius: the smaller peak intensity is compensated by a larger interaction region. Nonetheless, when w_0 is too large, q_0 becomes small and (5) and (6) lose their validity (see Fig. 3).

To be concrete, we now estimate the pressure that can be measured at a given ultraintense laser facility in a reasonable time span. As an example, we will consider the petawatt laser Vega that will be available in 2014 at the CLPU of Salamanca [21], having repetition rate as large as $r_r = 1\ \text{s}^{-1}$, with pulses of $\lambda_0 = 800$ nm, $\tau = 30$ fs and $E_{\text{pulse}} = 30$ J. Taking, e.g., $T = 300$ K, $w_0 = 20\ \mu$m, and a day run, $\Delta t = 1$ day, and assuming an efficiency $f = 0.5$ for $n = 1$, which is a realistic value for commercially available single photon detectors at $\lambda_1 = 800$ nm, we can compute the limiting pressure that can be measured within 3 standard deviations by taking $N_{\gamma,\text{det}}^{(1)} = 10$ in Eq. (6). We get $p_{\text{limit}} \simeq 0.3 \times 10^{-16} \frac{2}{\eta}$ Pa. This sensitivity should be corrected by a geometric efficiency factor, depending on the effective area of the detector.

In order to translate this result in terms of a pressure measurement, the actual value of η is needed. Such value will depend on the composition of the vacuum tube walls and pump elements, that can be measured at somewhat "higher" pressures as in Refs. [19,22], although when extrapolating the results of such measurements to the XHV regime extra hypotheses will be needed. In most cases, the value of η can be expected to be roughly $\eta \simeq 2$, as corresponding to just molecular hydrogen left in the chamber, or somewhat higher taking into account the possible contribution of other gases such as CO.

The angular cut imposed in the computation ensures that the detected photons will not be confused with those of the beam that do not undergo scattering, that would give no observable signal in the integration area for one day run. Such kind of background can also be avoided by measuring the $n = 2$ harmonic. From Eq. (6), the limiting pressure that can be measured by detecting $N^{(2)}_{\gamma,\mathrm{det}} = 10$ photons after one day run would be $p_{\mathrm{limit}} \simeq 0.6 \times 10^{-14} \frac{2}{\eta}$ Pa, if all the other parameters are taken as above except the efficiency, that can be as large as $f \simeq 0.6$ for $\lambda_2 \simeq 400$ nm in state-of-art single photon detectors. Thus, the detection of the $n = 2$ harmonic will provide an independent measurement of the pressure above the $\sim 10^{-14}$ Pa range for a one day run at Vega, complementary to the more sensitive measurement due to the $n = 1$ wave. Taken together, these measurements could be used for a kind of self-calibration of the whole procedure, that might also be complemented with a calibration using other known vacuum gauges for higher pressures. The result for the measurement of pressure as low as 10^{-14} Pa would then be highly reliable, provided that the detection is accurate enough and the noise level can be kept below the signal, which are feasible tasks with present technology as we discuss below.

Background analysis.—A source of noise is due to the dark counts of the detector, that can be kept below 10 s^{-1} in avalanche photodiodes featuring high efficiencies at the wavelengths discussed in this Letter. If we require that during each repetition the detection window is opened for a very short time, which can be as short as two nanoseconds with present technology, we can ensure that after the $\sim 10^5$ repetitions in the one day experiment at Vega the total dark counts would be unobservable. Such gating of the detector would also provide an efficient protection mechanism against the backscattered photons from the walls of the vacuum tube. A promising alternative could also be the use of superconducting single photon detectors [23,24], that can reduce the dark counts below 10^{-2} s^{-1} in both the visible and infrared ranges.

Detector gating would not be effective against Rayleigh background. Its relative importance can be roughly estimated by noticing that $N_{\gamma,\mathrm{Rayl}}/N_{\gamma,T} \propto \sigma_{\mathrm{Rayl}}/\sigma_T$, being $\sigma_{\mathrm{Rayl},T}$ the total cross sections for Rayleigh and Thomson scattering, respectively. Since $\sigma_{\mathrm{Rayl}}/\sigma_T \ll 1$ at optical wavelengths, the amount of Rayleigh photons is negligible. Similar considerations hold for Raman scattering since, typically, $\sigma_{\mathrm{Raman}} < \sigma_{\mathrm{Rayl}}$ [25].

Finally, we have verified that, at room temperature $T \simeq 300$ K and below, the thermal background, as given by Planck's law, can be made negligible in configurations of interest for this work by frequency filtering.

Validity of approximations.—We discuss now several approximations and assumptions that have been made in deriving our results. First of all, radiation reaction and quantum effects have been neglected in Eq. (2), which is a good approximation since $q^2 \ll \lambda_0/r_0$ and $nhc/\lambda_0 \ll m_e c^2$ in relevant situations. Moreover, (2) is valid for a plane wave. This means that the Gaussian beam radius should be larger than the transverse displacement of the electron which is typically of order $q\lambda$. Namely, the formalism is valid for $w_0 \gg q_0\lambda_0$ and cannot be used for diffraction limited beams (or, otherwise, electrons are swept away from the region of the pulse by the ponderomotive force, resulting in a much lower signal than the one derived from the expressions in Ref. [8], as happens in Ref. [15]). We have considered the radiating electrons as free. This is valid as long as the atomic potentials can be neglected in the presence of the laser beam, namely in the barrier suppression (BS) regime [26], which for hydrogen corresponds to $I > I_{\mathrm{BS}} = 1.4 \times 10^{14}$ $\mathrm{W/cm^2}$ [27]. Since this limiting value corresponds to $q \ll 1$ (it is $q \approx 0.01$ for $\lambda_0 = 800$ nm)—and $q \approx 1$ is related to the onset of relativistic effects—we conclude that the binding energy of the electrons does not play a role in the harmonic generation we have discussed. For the same reason, harmonic generation coming from electron-proton recombination is suppressed (and would be further suppressed if polarization were nonlinear) leaving relativistic Thomson scattering as the dominant process.

Notice that at ordinary temperatures the electron can be considered as initially at rest. Even if they are accelerated to relativistic velocities by the laser pulse, they do not get net energy from it under rather general conditions [28]. Therefore, they are again slow after the pulse has passed. Moreover, since electrons do not get large energies, a possible background coming from fast electrons reaching the detectors within gating time is negligible.

Finally, we have made a rough modeling considering square pulses and not taking into account the effects of the time envelope of the pulses. For short pulses—with a small or moderate number of light cycles—this approximation is not accurate, as it has been discussed both in classical [29,30] and quantum [31] frameworks. Depending on the precise form of the time envelope $g(t)$, Eq. (6) must be multiplied a factor of order 1. The easiest way to estimate this factor is to explicitly include a time dependence in q (see Ref. [20]), an approximation which is valid as long as $\frac{dg(t)}{dt} \ll \omega g(t)$, namely, if the time envelope changes slowly as compared to the light cycles [32].

Conclusions.—We have computed the amount and spatial distribution of the photons that are produced when a Gaussian laser pulse crosses a vacuum tube. With present detector and ultraintense laser technologies, this implies the possibility of measuring pressures as small as 10^{-16} Pa in a one-day experiment. This technique can be self-calibrated and highly reliable above the 10^{-14} Pa scale. Ultraintense lasers may be then able to push the limits for measuring a basic magnitude like pressure. A lower cost application can be the use of intermediate-intensity lasers as an alternative instrument of measuring high vacuum pressure in a nonextreme regime.

We thank J. Hernández-Toro, J. A. Pérez-Hernández, C. Ruiz, A. Peralta, and L. Roso for useful discussions. A. P. is supported by the Ramón y Cajal program. D. N. acknowledges support from Spanish MINECO through the FCCI. ACI-PROMOCIONA project (ACI2009-1008). D. T. thanks the InterTech group of Valencia Politechnical University for hospitality.

[1] P. A. Redhead, in *Foundations of Vacuum Science and Technology*, edited by J. M. Lafferty (Wiley, New York, 1998), p. 625.
[2] P. A. Redhead, CERN Rep. **99**, 213 (1999).
[3] J. Z. Chen, C. D. Suen, and Y. H. Kuo, J. Vac. Sci. Technol. A **5**, 2373 (1987).
[4] A. Calcatelli, Measurement (in press).
[5] H. Häffner, T. Beier, S. Djekić, N. Hermanspahn, H.-J. Kluge, W. Quint, S. Stahl, J. Verdú, T. Valenzuela, and G. Werth, Eur. Phys. J. D **22**, 163 (2003).
[6] G. A. Mourou, T. Tajima, and S. V. Bulanov, Rev. Mod. Phys. **78**, 309 (2006).
[7] J. H. Eberly and A. Sleeper, Phys. Rev. **176**, 1570 (1968).
[8] E. S. Sarachik and G. T. Schappert, Phys. Rev. D **1**, 2738 (1970).
[9] C. I. Castillo-Herrera and T. W. Johnston, IEEE Trans. Plasma Sci. **21**, 125 (1993).
[10] E. Esarey, S. K. Ride, and P. Sprangle, Phys. Rev. E **48**, 3003 (1993).
[11] Y. I. Salamin and F. H. M. Faisal, Phys. Rev. A **54**, 4383 (1996).
[12] S.-Y. Chen, A. Maxsimchuk, and D. Umstadter, Nature (London) **396**, 653 (1998); S. Y. Chen, A. Maksimchuk, E. Esarey, and D. Umstadter, Phys. Rev. Lett. **84**, 5528 (2000); M. Babzien *et al.*, Phys. Rev. Lett. **96**, 054802 (2006); T. Kumita *et al.*, Laser Phys. **16**, 267 (2006).
[13] O. Har-Shemesh and A. Di Piazza, Opt. Lett. **37**, 1352 (2012).
[14] S. L. Adler, Ann. Phys. (N.Y.) **67**, 599 (1971); E. B. Aleksandrov, A. A. Anselm, and A. N. Moskalev, Sov. Phys. JETP **62**, 680 (1985); Y. J. Ding and A. E. Kaplan, Phys. Rev. Lett. **63**, 2725 (1989); F. Moulin and D. Bernard, Opt. Commun. **164**, 137 (1999); D. Bernard, F. Moulin, F. Amiranoff, A. Braun, J. P. Chambaret, G. Darpentigny, G. Grillon, S. Ranc, and F. Perrone, Eur. Phys. J. D **10**, 141 (2000); G. Brodin, M. Marklund, and L. Stenflo, Phys. Rev. Lett. **87**, 171801 (2001); G. Brodin, L. Stenflo, D. Anderson, M. Lisak, M. Marklund, and P. Johannisson, Phys. Lett. A **306**, 206 (2003); V. I. Denisov, I. V. Krivchenkov, and N. V. Kravtsov, Phys. Rev. D **69**, 066008 (2004); T. Heinzl, B. Liesfeld, K.-U. Amthor, H. Schwoerer, R. Sauerbrey, and A. Wipf, Opt. Commun. **267**, 318 (2006); A. D. Piazza, K. Z. Hatsagortsyan, and C. H. Keitel, Phys. Rev. Lett. **97**, 083603 (2006); M. Marklund and P. K. Shukla, Rev. Mod. Phys. **78**, 591 (2006); A. Ferrando, H. Michinel, M. Seco, and D. Tommasini, Phys. Rev. Lett. **99**, 150404 (2007); D. Tommasini, A. Ferrando, H. Michinel, and M. Seco, Phys. Rev. A **77**, 042101 (2008).
[15] E. Lundstrom, G. Brodin, J. Lundin, M. Marklund, R. Bingham, J. Collier, J. T. Mendonça, and P. Norreys, Phys. Rev. Lett. **96**, 083602 (2006).
[16] B. King, A. D. Piazza, and C. H. Keitel, Nat. Photonics **4**, 92 (2010); M. Marklund, Nat. Photonics **4**, 72 (2010).
[17] D. Tommasini and H. Michinel, Phys. Rev. A **82**, 011803R (2010).
[18] M. Bregant *et al.* (PVLAS Collaboration), Phys. Rev. D **78**, 032006 (2008); G. Zavattini and E. Calloni, Eur. Phys. J. C **62**, 459 (2009); D. Tommasini, A. Ferrando, H. Michinel, and M. Seco, J. High Energy Phys. 11 (2009) 043; B. Dobrich and H. Gies, J. High Energy Phys. 10 (2010) 022.
[19] J. L. Abelleira-Fernández *et al.*, J. Phys. G **39**, 075001 (2012).
[20] See Supplemental Material at http://link.aps.org/supplemental/10.1103/PhysRevLett.109.253903 for will be inserted by publisher] for a discussion regarding the spectral distribution of the scattered radiation and the inclusion of the temporal dependence $g(t)$ in the calculations.
[21] http://www.clpu.es/en/.
[22] P. J. Bryant *et al.*, NASA Publication No. CR-324 (NASA Lewis Research Center, Cleveland, 1965).
[23] A. Korneev *et al.*, IEEE Trans. Appl. Supercond. **15**, 571 (2005).
[24] K. Smirnov, A. Korneev, O. Minaeva, A. Divochiy, M. Tarkhov, S. Ryabchun, V. Seleznev, N. Kaurova, B. Voronov, G. Gol'tsman, and S. Polonsky, J. Phys. Conf. Ser. **61**, 1081 (2007).
[25] N. B. Colthup, L. H. Daly, and S. E. Wiberley, *Introduction to Infrared and Raman Spectroscopy* (Academic Press, New York, 1990).
[26] N. B. Delone and V. P. Krainov, Usp. Fiz. Nauk **168**, 531 (1998).
[27] V. V. Strelkov, A. F. Sterjantov, N. Yu Shubin, and V. T. Platonenko, J. Phys. B **39**, 577 (2006).
[28] J. D. Lawson, IEEE Trans. Nucl. Sci. **26**, 4217 (1979); E. Esarey, C. B. Schroeder, and W. P. Leemans, Rev. Mod. Phys. **81**, 1229 (2009).
[29] G. A. Krafft, Phys. Rev. Lett. **92**, 204802 (2004).
[30] J. Gao, Phys. Rev. Lett. **93**, 243001 (2004); Y. Tian, W. Yu, P. Lu, V. Senecha, Y. Cang, H. Xu, D. Deng, R. Li, and Z. Xu, Opt. Commun. **261**, 104 (2006); Y. Tian, Y. Zheng, Y. Lu, and J. Yang, Optik (Stuttgart) **122**, 1373 (2011).
[31] F. Mackenroth and A. D. Piazza, Phys. Rev. A **83**, 032106 (2011).
[32] P. Gibbon, *Short Pulse Laser Interaction with Matter* (Imperial College Press, London, 2007).